· Clinical Research ·

Altered amplitudes of low-frequency fluctuations in primary open angle glaucoma patients: a resting-state fMRI study

Yi Huang[1], Hong–Dou Luo[1], Yong–Qiang Shu[2], Feng Ouyang[2], Yu–Ning Song[1], Yuan–Yuan Wang[2], Xue–Qing Yu[1], Chan Xiong[1], Lu Yang[1], Xu Zhang[1]

[1]Affiliated Eye Hospital of Nanchang University, Jiangxi Medical College, Nanchang University, Jiangxi Research Institute of Ophthalmology and Visual Science, Jiangxi Provincial Key Laboratory for Ophthalmology, Jiangxi Clinical Research Center for Ophthalmic Disease, Nanchang 330006, Jiangxi Province, China

[2]Department of Radiology, the First Affiliated Hospital, Jiangxi Medical College, Nanchang University; PET Center, the First Affiliated Hospital of Nanchang University, Nanchang 330006, Jiangxi Province, China

Co-first Authors: Yi Huang and Hong-Dou Luo

Correspondence to: Xu Zhang. Affiliated Eye Hospital of Nanchang University, Nanchang 330006, Jiangxi Province, China. xuzhang19@163.com

Received: 2025-03-07 Accepted: 2025-08-08

Abstract

● **AIM:** To study the relationships between amplitude of low-frequency fluctuations (ALFF) changes and clinical ophthalmic parameters in patients with primary open angle glaucoma (POAG) and analyze the diagnostic value of ALFF.

● **METHODS:** Twenty-four POAG patients and 24 healthy controls (HCs) underwent resting-state functional magnetic resonance imaging (rs-fMRI). Nonparametric rank-sum tests were used to compare the ALFF values in the slow-4 and slow-5 bands, and Spearman or Pearson correlation analysis was used to assess the correlation between ALFF changes and clinical ophthalmic parameters in POAG patients. Receiver operating characteristic (ROC) curves were used to evaluate the diagnostic performance of the ALFF.

● **RESULTS:** There were 16 males in POAG patients (median age 48y) and 12 males in HCs (median age 39y). Compared with HCs, POAG patients presented increased or decreased ALFF values in different brain regions, and similar changes were observed in mild POAG patients. The ALFF values were correlated with retinal nerve fiber layer (RNFL) thickness, inner limiting membrane-retinal pigment epithelium thickness changes and the degree of visual field defects. Analysis of the diagnostic value of the ALFF *via* ROC curves revealed that the right medial frontal gyrus [area under the curve (AUC)=0.9063] and superior frontal gyrus (AUC=0.9097) had better diagnostic value than did the optic disc area (AUC=0.8019), visual field index (VFI%, AUC=0.8988) and macular parameters.

● **CONCLUSION:** POAG patients present altered cortical function that is significantly correlated with the optic nerve and retinal thickness and had good diagnostic value, which may reflect the underlying neuropathological mechanism of POAG.

● **KEYWORDS:** primary open angle glaucoma; resting-state functional magnetic resonance imaging; low-frequency amplitude; neurodegenerative disease

DOI:10.18240/ijo.2026.02.11

Citation: Huang Y, Luo HD, Shu YQ, Ouyang F, Song YN, Wang YY, Yu XQ, Xiong C, Yang L, Zhang X. Altered amplitudes of low-frequency fluctuations in primary open angle glaucoma patients: a resting-state fMRI study. *Int J Ophthalmol* 2026;19(2):291-301

INTRODUCTION

Glaucoma is one of the main eye diseases causing blindness worldwide, and ocular hypertension is considered the most important pathogenic factor in glaucoma. In addition, mechanical, vascular and immunological[1-3], genetic[4], and inflammatory[5] have been shown to be involved in the lesion process.

Primary open angle glaucoma (POAG) is the most common type of open angle glaucoma, but patients with POAG may continue to lose vision even if the intraocular pressure is effectively controlled. Therefore, further study of the pathogenesis of this disease is necessary. Currently, neuropathological studies suggest that POAG is a neurodegenerative disease[1,6]. Multiple studies have suggested that POAG lesions are not restricted to the visual system but also involve neurodegenerative lesions in multiple brain regions[7-8]. Magnetic resonance imaging (MRI)[9], diffusion kurtosis imaging[10], diffusion tensor imaging[11] and other imaging technologies are new methods used to detect glaucoma lesions in the brain and provide evidence for the presence of neurodegenerative changes in the brain in glaucoma patients. These observations suggest that glaucoma results in abnormal changes in the brain before severe loss of vision[12]. Functional magnetic resonance imaging (fMRI) is widely used in various neurodegenerative diseases involving the central nervous system, and it is also suitable for exploring the mechanism of POAG.

The amplitude of low-frequency fluctuations (ALFF) indicates the intensity of low-frequency oscillations and has been shown to be a valuable parameter reflecting the intensity of spontaneous neural activity. Optic nerve damage is the most common feature of POAG, and previous functional studies of glaucoma have tended to correlate nerve damage with abnormal brain activity. In recent studies on ALFF, Chai *et al*[13] studied the changes in surface-based ALFF and low-frequency fluctuation fractional amplitude (fALFF) in POAG patients and investigated their relationships with visual function and molecular spectra. Wang *et al*[14] analyzed the changes in the functional connectivity patterns of resting-state and dynamic brain networks and then analyzed their relationships with clinical variables. Li *et al*[15] used resting-state ALFF and diffusion tensor image analysis along the perivascular space (DTIALPS) to investigate the correlation between brain region changes and clinical ophthalmic parameters. However, the focus of these studies was on imaging, and few studies have analyzed clinical ophthalmic parameters, with some even showing only mean deviation (MD) values. At present, many studies have shown that macular lesions are associated with the progression of POAG[16] and that the parameters are deranged very early in glaucoma[17]. However, no studies have simultaneously analyzed the associations between optic nerve damage and macular lesions in POAG patients or ALFF values. Therefore, in our study, we provide a detailed analysis of macular changes as well as changes in nerve fiber thickness to better analyze the diagnostic value of ALFF. Furthermore, ALFF is similar to fluctuations in neurophysiological, dynamic and metabolic parameters, and decreased ALFF may indicate dynamic and metabolic disturbances in those brain regions. In this study, we investigated the relationships between ALFF values and clinical data in POAG patients by studying the slow-4 and slow-5 bands because they had higher test-retest reliability for ALFF measurements.

In our previous study, we reported that POAG patients presented altered degree centrality values, which were associated with cup-to-disc (C/D) ratios, intraocular pressure (IOP) and pattern standard deviation (PSD)[16]. Therefore, we further analyzed the correlation between POAG ophthalmic findings and spontaneous neural activity in the brain to explore the diagnostic value of ALFF in different brain regions of POAG patients.

PARTICIPANTS AND METHODS

Ethical Approval This retrospective observational study was approved by the Medical Ethics Committee of Nanchang University (ethics number: YLP201810002). The study adhered to the tenets of the Declaration of Helsinki (1964). Written informed consent was provided by all participants.

Participants In this study, 24 POAG patients (47 eyes) diagnosed between 2018 and 2023 were included in the study group, and 24 healthy volunteers (48 eyes) matched for age, sex, handedness and education level were included in the control group.

The inclusion criteria for POAG patients were as follows: 1) met the diagnostic criteria for POAG; 2) were right-handed[18]; 3) had no other optic neuropathy, ocular disease, intraocular disease, ocular surgery history or other diseases affecting the visual field; 4) had no foreign body implants; 5) had no brain MRI data showing significantly abnormal brain parenchyma; 6) had no history of congenital or acquired disease or drug use disorders.

All healthy controls (HCs) met the following criteria: 1) presence of other ocular diseases or organic conditions affect the visual pathway, history of glaucoma or significant eye diseases, prior glaucoma surgery[19]; 2) MRI of the head showing no abnormal visual pathway or brain parenchyma; 3) no contraindications to MRI; 4) normal neurological and mental health with no migraine. The clinical history of every patient was collected in detail.

Ophthalmic Examination The clinical diagnostic criteria for POAG were as follows: an open anterior chamber angle, visual field defects, an abnormal optic disc, and increased intraocular pressure. The eyes of POAG patients were divided into mild (MD$\geq$-6 dB), moderate (-12<MD<-6 dB), and severe (MD$\leq$-12 dB) groups according to the MD[20]. The circumpapillary retinal nerve fiber layer thickness (cpRNFLT) partition[21] and the total retina thickness (thickness from the internal limiting membrane to the retinal pigment epithelium; ILM-RPET) partition[22] are shown in Figure 1. Locations of the retinal nerve fiber layer thickness (RNFLT): superior (RNFL-ST), inferior (RNFL-IT), nasal (RNFL-NT), and temple (RNFL-TT). Locations of the total retina thickness (ILM-RPET): outer superior retina (ROS), outer nasal retina (RON), outer inferior retina (ROI), outer temporal retina (ROT), inner superior retina (RIS), inner nasal retina (RIN), inner inferior retina (RII), inner temporal retina (RIT), and central retina (RC).

MRI Data Acquisition All MRI data were collected on a Siemens Trio 3.0 T scanner with an 8-channel phased array head coil at the First Affiliated Hospital of Nanchang University, China. Each subject lay in the supine position, and their head was comfortably secured in a neutral position with a belt and foam pad during the MRI scan.

We obtained high-resolution brain structural images for each subject *via* a T1-weighted 3D magnetization-prepared rapid gradient-echo sequence.

FMRI Data Preprocessing All fMRI functional images were preprocessed *via* Brain Imaging Data Processing Assistant and Analysis Toolbox (http://rfmri.org/dpabi) software implemented in MATLAB 2013a (MathWorks, Natick, MA, USA), and most functions were based on Statistical Parametric Mapping 12 software (http://www.fil.ion.ucl.ac.uk/spm/)[23].

Statistical Analysis Statistical Package for Social Sciences 25.0 software (IBM, Armonk, NY, USA) and GraphPad Prism 9.0 software were used for statistical analysis. The general data of the POAG patients and HCs and the differences in the ALFF between the POAG patients (grouped by MD) were analyzed *via* nonparametric rank-sum tests[24]. For each frequency band, a two-sample t test was performed to compare the ALFF values *via* Gaussian random field (GRF) theory [voxel-level P<0.001, GRF correction, cluster-level P<0.01]. In addition, Pearson (nonnormality test) or Spearman (nonnormality test) correlation analysis was used to look for associations between the ALFF and clinical level, with a threshold of P<0.05 indicating statistical significance. Finally, receiver operating characteristic (ROC) curves were used to assess the diagnostic performance of ALFF values in different brain regions for detecting POAG.

RESULTS

Participant Characteristics A total of 24 POAG patients and 24 HCs were included. There were no significant differences in the general statistical data (age, sex, handedness, education; P>0.05, r<0.1; Table 1). POAG patients were grouped by MD, and there were no significant differences among the groups in terms of age (P=0.245), RNFL-NT (P=0.633), disc area (P=0.916), RC (P=0.169), ROI (P=0.314), ROT (P=0.177), or brain interval. There were significant differences in visual field index (VFI%), PSD, RNFL-ST, RNFL-IT, RNFL-TT, mean RNFL, average C/D ratio, vertical C/D ratio, rim area, RIS, RIN, RON, RII and RIT between mild and severe POAG patients. There were significant differences between the mild and moderate groups in PSD, RNFL-IT, RNFL-TT, and mean RNFL. There were significant differences between the moderate and severe groups in VFI%, RIS, RIN and RIT (Table 2). when the eyes were grouped as covariates, we found that the MD values varied significantly between the groups (P=0.025; Figure 2A), but the effect size was small (r=0.048), and there was no significant difference in the baseline criteria between the two eyes.

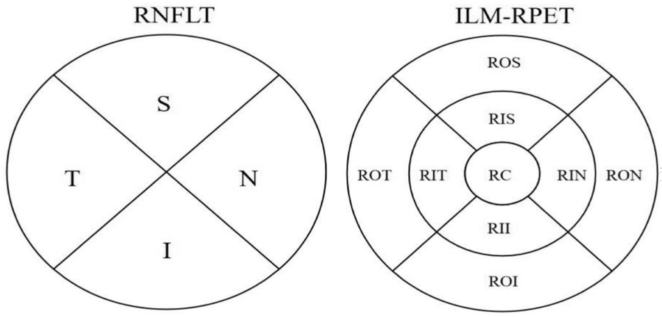

Figure 1 Locations of the retinal nerve fiber layer thickness (RNFLT) and total retina thickness (ILM-RPET) S: Superior; I: Inferior; N: Nasal; T: Temple; ILM-RPET: Thickness from the internal limiting membrane to the retinal pigment epithelium; ROS: Outer superior retina; RON: Outer nasal retina; ROI: Outer inferior retina; ROT: Outer temporal retina; RIS: Inner superior retina; RIN: Inner nasal retina; RII: Inner inferior retina; RIT: Inner temporal retina; RC: Central retina.

Table 1 General comparison between the POAG and HC groups

Parameters	POAG	HCs	Z	P
Age (y)	48 (35, 68)	39.00 (30.25, 59.25)	-1.788	0.074
Sex (M/F)	16/8	12/12	-1.167	0.243
Handedness	24 right	24 right	-	>0.99
Education (y)	7 (7, 16)	7 (7, 12)	-1.879	0.06

POAG: Primary open angle glaucoma; HCs: Healthy controls.

ALFF Differences Compared with those in HCs, the slow-4 band in POAG patients presented increased ALFF values in the left lingual gyrus (LING.L), RC, and right postcentral gyrus (PoCG.R) and decreased ALFF values in the right inferior frontal gyrus (IFG.R; P<0.0001). In the slow-5 band, POAG patients had increased ALFF values in the LING.L, RC, and the right medial frontal gyrus (MedFG.R) and decreased ALFF values in the superior frontal gyrus (SFG; P<0.0001; Tables 3 and 4, Figure 2D, 2E). POAG patients were divided into left and right eye groups, and no significant difference in ALFF values was found between the two groups (P>0.05; Figure 2C). The same changes in ALFF values in the above brain areas were found in mild POAG patients (P<0.0001; Figure 2F). POAG patients were divided into three groups according to their MD: mild, moderate and severe. We detected corresponding changes in brain regions with changing MD values, but there was no statistically significant difference in the ALFF values among the groups (P>0.05; Figure 2G).

Correlation Analysis

Correlation analysis of ophthalmic parameters in patients with mild POAG and ALFF values Although we found that multiple groups of clinical parameters associated with POAG are related to the ALFF in the slow-4 band and slow-5 band, we only explored the relationships between multiple clinical ophthalmic parameters in the same brain region.

We found that, in the slow-4 band, the ALFF values of the LING.L were positively correlated with VFI% (r=0.617,

Table 2 General clinical data of the eyes of POAG patients classified by MD

Parameters	Mild (*n*=14)	Moderate (*n*=11)	Severe (*n*=22)	*Z*	*P*
Age (y)	43.50 (35.00, 69.00)	54.00 (32.00, 58.00)	56.00 (41.25, 69.00)	2.963	0.245
VFI%	98.5 (88.25, 99.00)[b]	83.00 (80.00, 89.00)[b]	11.50 (3.00, 44.00)	27.617	0.000
PSD	2.04 (1.35, 3.32)[b]	7.71 (5.33, 8.75)[a]	5.97 (3.13, 10.34)	10.487	0.004
RNFL-ST	92.00 (72.25, 109.25)[b]	69.00 (60.00, 90.00)	63.00 (57.50, 80.00)	8.106	0.009
RNFL-NT	61.00 (49.00, 71.00)	59.00 (48.00, 62.00)	63.00 (54.00, 67.50)	1.392	0.633
RNFL-IT	91.00 (64.75, 126.25)	64.00 (56.00, 73.00)[a]	66.00 (53.00, 73.6)[a]	8.132	0.013
RNFL-TT	73.00 (50.25, 89.25)	44.00 (35.00, 51.00)[a]	52.00 (41.75, 60.00)[a]	9.101	0.002
RNFL-mean	79.50 (68.25, 95.25)	59.00 (52.00, 63.00)[a]	60.00 (54.25, 68.25)[a]	10.007	0.002
AVG C/D	0.74 (0.59, 0.80)	0.75 (0.69, 0.83)	0.87 (0.80, 0.92)[a]	12.338	0.004
V C/D	0.73 (0.50, 0.76)	0.75 (0.70, 0.84)	0.88 (0.78, 0.90)[a]	10.814	0.007
Rim area	0.95 (0.71, 1.18)	0.80 (0.59, 0.91)	0.53 (0.38, 0.81)[a]	13.592	0.002
Disc area	2.12 (1.68, 2.39)	2.13 (1.67, 2.58)	2.10 (1.88, 2.43)	0.754	0.916
RC	259.00 (244.75, 264.25)	249.00 (241.00, 265.00)	235.00 (220.50, 266.50)	2.854	0.169
RIS	316.00 (306.50, 322.25)[b]	309.00 (282.00, 329.00)[b]	279.50 (260.75, 301.75)	10.239	0.001
ROS	268.00 (261.50, 278.50)[b]	257.00 (237.00, 284.00)	250.00 (223.75, 272.25)	3.113	0.046
RIN	316.00 (307.75, 323.25)[b]	310.00 (289.00, 329.00)[b]	279.50 (263.00, 305.75)	12.350	0.001
RON	283.00 (269.50, 299.00)	277.00 (244.00, 299.00)	266.50 (233.25, 285.25)	4.612	0.113
RII	301.50 (286.75, 311.75)[b]	304.00 (272.00, 317.00)	272.50 (257.75, 297.00)	7.441	0.009
ROI	248.50 (231.00, 260.25)	242.00 (224.00, 252.00)	239.50 (218.25, 249.50)	3.255	0.314
RIT	297.50 (289.00, 308.75)[b]	293.00 (277.00, 306.00)[b]	268.00 (255.50, 288.25)	9.898	0.002
ROT	249.50 (244.00, 259.00)	246.00 (234.00, 259.00)	242.00 (223.75, 257.00)	3.340	0.177

[a]$P<0.05$ compared with the mild group; [b]$P<0.05$ compared with the severe group. VFI: Visual field index; PSD: Pattern standard deviation; RNFL-ST: Retinal nerve fiber layer superior thickness; RNFL-NT: Retinal nerve fiber layer nasal thickness; RNFL-IT: Retinal nerve fiber layer inferior thickness; RNFL-TT: Retinal nerve fiber layer temporal thickness; RNFL-mean: Mean retinal nerve fiber layer thickness; AVG C/D: Average cup-disc ratio; V C/D: Vertical cup-disc ratio; RC: Central retina; RIS: Inner superior retina; ROS: Outer superior retina; RIN: Inner nasal retina; RON: Outer nasal retina; RII: Inner inferior retina; ROI: Outer inferior retina; RIT: Inner temporal retina; ROT: Outer temporal retina.

Table 3 Differences in ALFF values in the slow-4 band between POAG patients and healthy controls

Brain regions	MNI coordinates, mm			Cluster size	*t*-value
	x	y	z		
Left lingual gyrus	-18	-81	-6	206	5.0665
Right calcarine	24	-48	6	64	4.4131
Right inferior frontal gyrus	21	33	6	110	-4.7444
Right postcentral gyrus	27	-39	57	101	5.024

GRF correction, voxel level: $P<0.001$, cluster level: $P<0.01$. ALFF: Amplitude of low-frequency fluctuations; POAG: Primary open angle glaucoma; GRF: Gaussian random field; MNI: Montreal Neurological Institute.

Table 4 Differences in ALFF in the slow-5 band between POAG patients and healthy controls

Brain regions	MNI coordinates, mm			Cluster size	*t*-value
	x	y	z		
Left lingual gyrus	-18	-81	-6	96	4.9416
Right calcarine	15	-48	0	71	4.6382
Right medial frontal gyrus	6	57	18	121	-5.306
Superior frontal gyrus	-24	51	21	107	-4.5134

GRF correction, voxel level: $P<0.001$, cluster level: $P<0.01$. ALFF: Amplitude of low-frequency fluctuations; POAG: Primary open angle glaucoma; GRF: Gaussian random field; MNI: Montreal Neurological Institute.

P=0.009) and negatively correlated with PSD (r=-0.710, P=0.004; Figure 3A), the ALFF values of the right calcarine (CAL.R) were positively correlated with VFI% (r=0.736, P=0.003) and negatively correlated with PSD (r=-0.604, P=0.022; Figure 3B); the ALFF values of the IFG.R were negatively correlated with MD (r=-0.662, P=0.010) and disc area (r=-0.547, P=0.043; Figure 3C). The ALFF values of the SFG were positively correlated with MD (r=0.635, P=0.015) and the disc area (r=0.536, P=0.048; Figure 3D). In the slow-5 band, the ALFF values of the LING.L in the POAG group were positively correlated with VFI% (r=0.674, P=0.008; Figure 3E), the RIN (r=0.624, P=0.017) and the RIT (r=0.576, P=0.031; Figure 3F) and negatively correlated with PSD (r=-0.710, P=0.004; Figure 3E). The ALFF values of the CAL.R were negatively correlated with PSD (r=-0.542, P=0.045) and positively correlated with VFI% (r=0.585, P=0.028; Figure 3G), ROS (r=0.659, P=0.010) and RON (r=0.609, P=0.021; Figure 3H).

Besides, in the slow-4 band, the ALFF values of the LING.L in the mild POAG group was positively correlated with RIN (r=0.538, P=0.047), the ALFF values of the PoCG.R were positively correlated with RC (r=0.573, P=0.032). In the

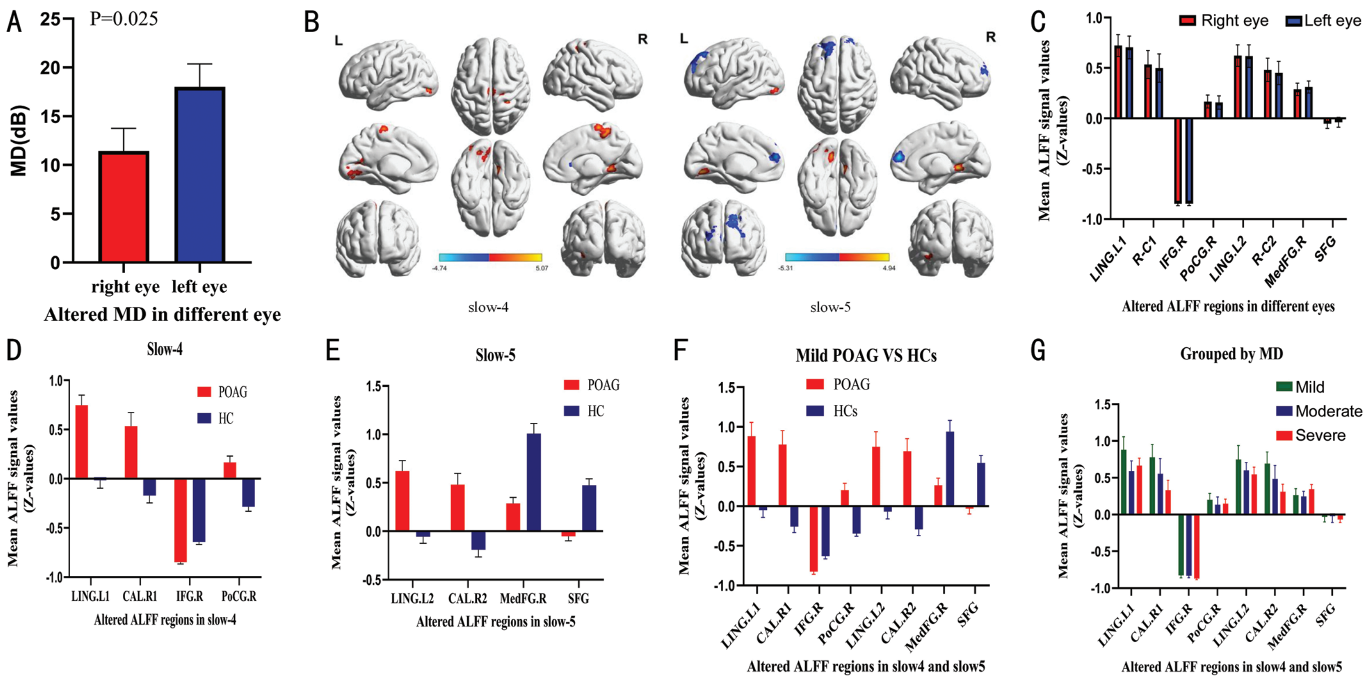

Figure 2 Differential analysis of brain regions and MD in POAG patients A: Comparison of MD changes in right/left eyes; B: Significant differences in spontaneous brain activity between patients with POAG and HCs. The sizes of the spots represent the degree of quantitative changes. Different brain regions were detected in the LING.L, CAL.R, IFG.R, PoCG.R, MedFG.R and SFG. The blue areas denote that patients with POAG exhibit lower ALFF values in brain areas than HCs do, and the red areas denote brain regions with higher ALFF values. C: Intergroup ALFF comparisons of POAG grouped by different eyes. D, E: Means of altered spontaneous brain activity compared between patients with POAG and HCs in the slow-4 and slow-5 groups. F: Comparison of ALFF changes in mild POAG patients with HCs. G: Intergroup ALFF comparison of POAG patients grouped by MD. The statistical threshold was set at a voxel with $P<0.05$ for the nonparametric rank sum set and standard error of the mean. MD: Mean deviation; POAG: Primary open angle glaucoma; HCs: Healthy controls; LING.L1: Left lingual gyrus in slow-4 band; LING.L2: Left lingual gyrus in slow-5 band; CAL.R1: Right calcarine in slow-4 band; CAL.R2: Right calcarine in slow-5 band; IFG.R: Right inferior frontal gyrus; PoCG.R: Right postcentral gyrus; MedFG.R: Right medial frontal gyrus; SFG: Superior frontal gyrus; ALFF: Amplitude of low-frequency fluctuations.

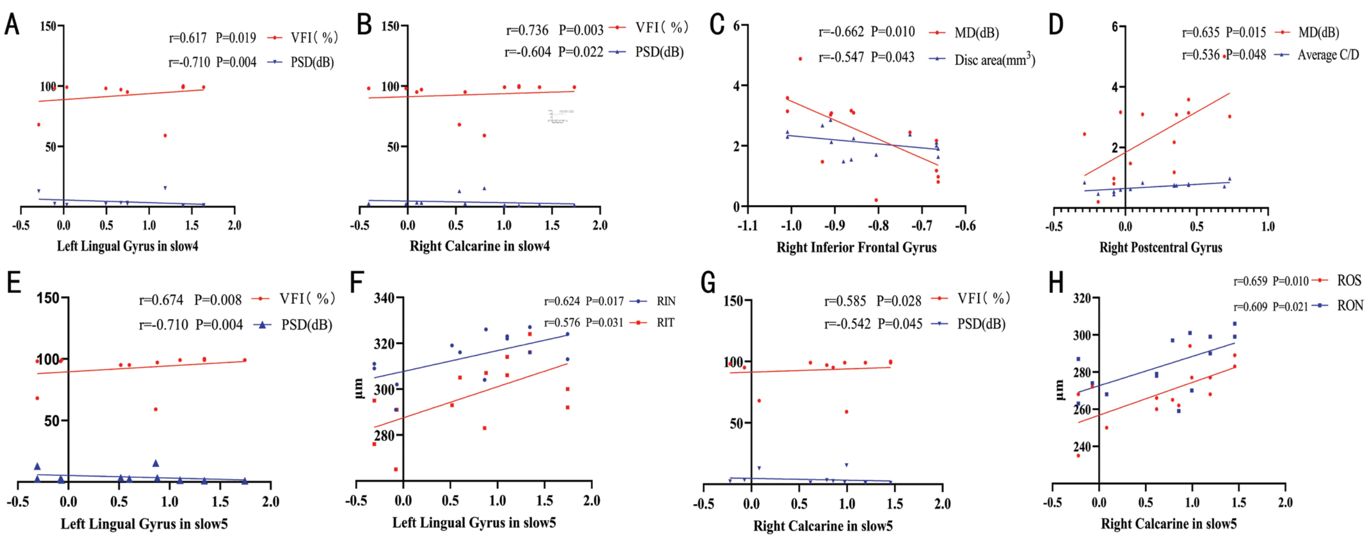

Figure 3 Relationships between ALFF variation and clinical variables in mild POAG patients For the slow-4 band, the ALFF values of the LING.L in the POAG group was positively correlated with VFI% and negatively correlated with PSD (A); CAL.R was positively correlated with VFI% and negatively correlated with PSD (B). The IFG.R was negatively correlated with MD and the disc area (C); The PoCG.R was positively correlated with MD and the average C/D (D). For the slow-5 band, the ALFF values of the LING.L in the POAG group was positively correlated with VFI% (E), the RIN, and the RIT (F) and negatively correlated with PSD (E) and CAL.R was positively correlated with VFI% (G) and ROS, RON (H) and negatively correlated with PSD (G). ALFF: Amplitude of low-frequency fluctuations; POAG: Primary open angle glaucoma; LING.L: Left lingual gyrus; VFI: Visual field index; PSD: Pattern standard deviation; CAL.R: Right calcarine; IFG.R: Right inferior frontal gyrus; C/D: Cup-disc ratio; RIN: Inner nasal retina; RIT: Inner temporal retina; ROS: Outer superior retina; RON: Outer nasal retina.

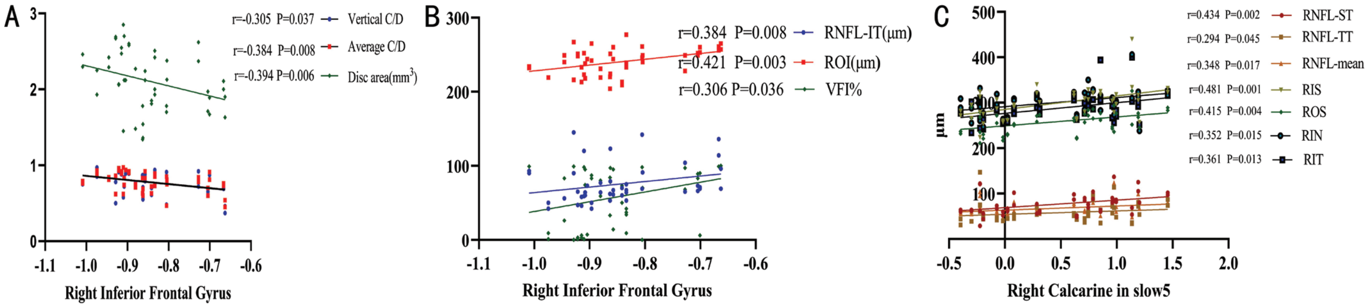

Figure 4 Relationships between ALFF variation and binocular clinical variables For the slow-4 band, the ALFF values of the IFG.R was negatively correlated with the vertical C/D, average C/D and disc area (A), which was positively correlated with the RNFL-IT, ROI and VFI% (B). In the slow-5 band, the ALFF values of the CAL.R was positively correlated with the RNFL-ST, RNFL-TT, RNFL-mean, RIS, ROS, RIN, and RIT (C). ALFF: Amplitude of low-frequency fluctuations; IFG.R: Right inferior frontal gyrus; C/D: Cup-disc ratio; RNFL-IT: Retinal nerve fiber layer inferior thickness; ROI: Outer inferior retina; VFI: Visual field index; CAL.R: Right calcarine; RNFL-ST: Retinal nerve fiber layer superior thickness; RNFL-TT: Retinal nerve fiber layer temporal thickness; RNFL-mean: Mean retinal nerve fiber layer thickness; RIS: Inner superior retina; ROS: Outer superior retina; RIN: Inner nasal retina; RIT: Inner temporal retina.

slow-5 band, the ALFF values of the CAL.R were negatively correlated with age (r=-0.686, P=0.007) and average C/D (r=-0.554, P=0.040), the ALFF values of the MedFG.R were positively correlated with the RNFL-NT (r=0.559, P=0.038). The ALFF values of the SFG were negatively correlated with the RNFL-TT (r=0.542, P=0.045).

Correlation analysis of eye parameters and ALFF in POAG patients For the slow-4 band, the ALFF values of the IFG.R was negatively correlated with the vertical C/D (r= -0.384, P=0.008), average C/D (r=-0.384, P=0.008), disc area (r=-0.394, P=0.006; Figure 4A), RNFL-IT (r=0.384, P=0.008), and ROI (r=0.421, P=0.003; Figure 4B). For the slow-5 band, the ALFF values of the CAL.R were positively correlated with RNFL-ST (r=0.434, P=0.002), RNFL-TT (r=0.294, P=0.045), RNFL-mean (r=0.348, P=0.017), RIS (r=0.481, P=0.001), ROS (r=0.415, P=0.004), RIN (r=0.352, P=0.015) and RIT (r=0.361, P=0.013; Figure 4C).

Besides, for the slow-4 band, the ALFF values of the LING.L in the POAG group were positively correlated with RNFL-ST (r=0.300, P=0.040), the ALFF values of the CAL.R were positively correlated with RNFL-ST (r=0.378, P=0.009) and disc area (r=0.370, P=0.011), the ALFF values of the PoCG.R were positively correlated with age (r=0.316, P=0.031) and disc area (r=0.320, P=0.028).

For the slow-5 band, the ALFF values of the LING.L in the POAG group were negatively correlated with age (r=-0.317, P=0.030), the ALFF values of the CAL.R were negatively correlated with age (r=-0.422, P=0.003), the ALFF values of the MedFG.R were positively correlated with RNFL-NT (r=0.357, P=0.014), the ALFF values of the SFG were negatively correlated with the average C/D ratio (r=-0.331, P=0.023).

Correlation analysis of right/left eye parameters and ALFF in POAG patients To further explore the relationship between the different variations in the right/left brain regions of POAG patients and the difference in the severity of disease in the right/left eye of POAG patients, we assessed the correlation of the POAG left/right eye ophthalmic parameters with bilateral differential brain regions. When we analyzed the correlations between ophthalmic parameters in the right eye and brain regions with abnormalities in the slow-4 band, we found that the ALFF values of the IFG.R was negatively correlated with the vertical C/D ratio (r=-0.416, P=0.043) and disc area (r=-0.466, P=0.022; Figure 5A). For the slow-5 band, the ALFF values of the CAL.R in the POAG group were positively correlated with RNFL-ST (r=0.519, P=0.009), RNFL-mean (r=0.476, P=0.019), RIS (r=0.453, P=0.026), ROS (r=0.487, P=0.016), RIN (r=0.453, P=0.026), and RON (r=0.444, P=0.030; Figure 5B).

Relationships between ALFF variation and clinical variables in the left eye. For the slow-4 band, the ALFF values of the CAL.R were positively correlated with the RIS (r=0.481, P=0.020) and RIT (r=0.423, P=0.045; Figure 5C). the ALFF values of the MedFG.R were positively correlated with VFI% (r=-0.578, P=0.004), MD (r=0.594, P=0.003) and RNFL-NT (r=0.530, P=0.009; Figure 5D).

The larger the MD value and the smaller the VFI value are, the greater the ALFF value in the MedFG.R, and the MedFG.R may be associated with glaucoma injury; however, in our study, RNFL-NT values were found to be positively correlated with ALFF, which may be associated with a small correlation between RNFL-NT and glaucoma injury or the presence of optic disc hemorrhage or edema later in disease progression.

More findings on the correlation of other POAG clinical parameters with ALFF can be found. When analyzing the correlation between ophthalmic parameters in the right eye and brain regions with abnormalities in the slow-4 band, we found that the ALFF values of the CAL.R were positively correlated

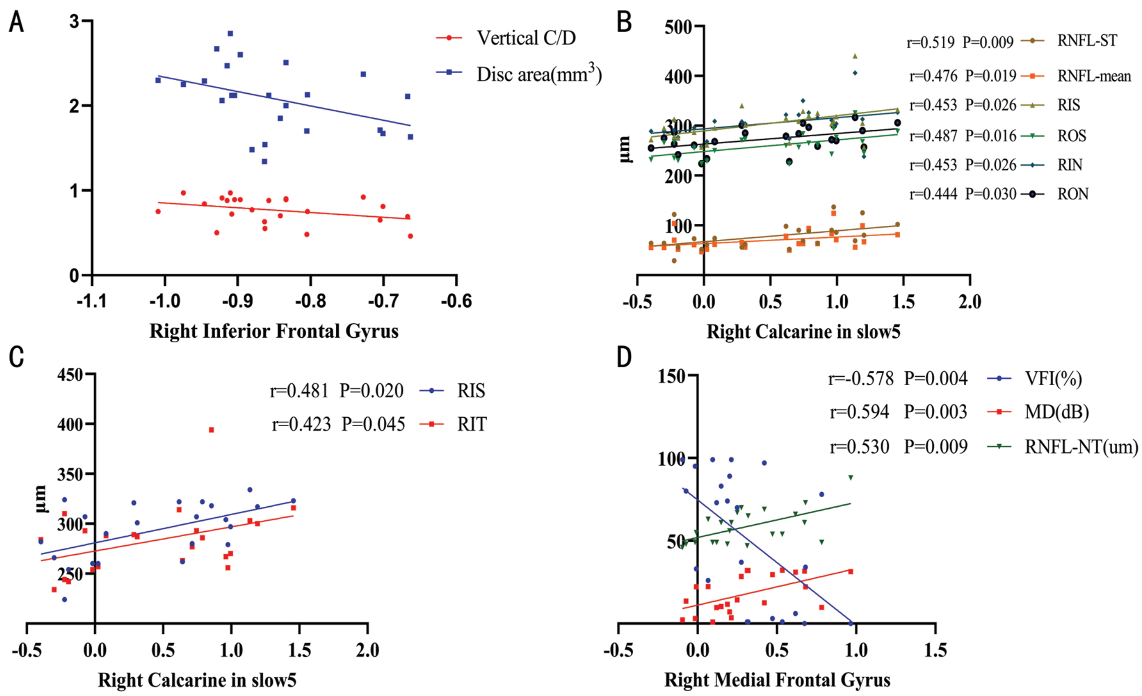

Figure 5 Relationships between ALFF variation and clinical variables in different eyes In the right eye, for the slow-4 band, the ALFF values of the IFG.R was negatively correlated with the vertical C/D and disc area (A). In the slow-5 band, the ALFF values of the CAL.R in the POAG group was positively correlated with the RNFL-ST, RNFL-mean, RIS, ROS, RIN and RON (B). In the left eye, for the slow-5 band, the ALFF values of the CAL.R was positively correlated with the RIS and RIT (C); the ALFF values of the MedFG.R was positively correlated with VFI% and positively correlated with MD and RNFL-NT (D). ALFF: Amplitude of low-frequency fluctuations; IFG.R: Right inferior frontal gyrus; C/D: Cup-disc ratio; CAL.R: Right calcarine; POAG: Primary open angle glaucoma; CAL.R: Right calcarine; RNFL-ST: Retinal nerve fiber layer superior thickness; RNFL-mean: Mean retinal nerve fiber layer thickness; RIS: Inner superior retina; ROS: Outer superior retina; RIN: Inner nasal retina; RON: Outer nasal retina; RIS: Inner superior retina; RIT: Inner temporal retina; MedFG.R: Right medial frontal gyrus; VFI: Visual field index; MD: Mean deviation; RNFL-NT: Retinal nerve fiber layer nasal thickness.

with RNFL-ST (*r*=0.496, *P*=0.014), the ALFF values of the PoCG.R were positively correlated with the vertical C/D ratio (*r*=0.433, *P*=0.035). For the slow-5 band, the ALFF values of the RC in the POAG group were negatively correlated with age (*r*=-0.415, *P*=0.044).

Relationship between ALFF variation and clinical variables in the left eye. For the slow-4 band, the ALFF values of the LING.L in the POAG group were negatively correlated with RNFL-NT (*r*=-0.452, *P*=0.030). The ALFF values of the CAL.R were positively correlated with the disc area (*r*=0.482, *P*=0.020). The ALFF values of the IFG.R were positively correlated with ROI (*r*=0.546, *P*=0.007). The ALFF values of the PoCG.R were positively correlated with the RIS (*r*=0.417, *P*=0.048). For the slow-5 band, the ALFF values of the LING. L in the POAG group were negatively correlated with RNFL-NT (*r*=-0.430, *P*=0.041). The ALFF values of the CAL.R were negatively correlated with age (*r*=-0.430, *P*=0.041).

Receiver Operating Characteristic Curve According to our findings, the difference in ALFF between the POAG patient and HCs may provide a reference for the early diagnosis of POAG. Therefore, we used ROC curves to analyze ALFF values in different brain regions and compared them with several clinical ophthalmic parameters to assess their diagnostic value; the larger the area under the curve (AUC) was, the greater the diagnostic value. ROC curve analysis was performed only if there were at least 2 occurrences of associated clinical parameters in different correlation analyses of the same brain region.

The AUCs were as follows: in the slow-4 band, the LING.L AUC was 0.8611 [*P*<0.0001, 95% confidence interval (CI): 0.7997-0.9625], the CAL.R AUC was 0.8125 (*P*=0.0002, 95%CI: 0.6825-0.9425), the IFG.R AUC was 0.901 (*P*<0.0001, 95%CI: 0.8170-0.9851), and the PoCG.R AUC was 0.8854 (*P*<0.0001, 95%CI: 0.7899-0.9809). In the slow-5 band, the LING.L AUC was 0.8628 (*P*<0.0001, 95%CI: 0.7597-0.9660), the CAL.R2 AUC was 0.8385 (*P*<0.0001, 95%CI: 0.7296-0.9474), the MedFG.R AUC was 0.9063 (*P*<0.0001, 95%CI: 0.8262-0.9863), the SFG AUC was 0.9097 (*P*<0.0001, 95%CI: 0.8236-0.9958; Figure 6A);the RIT AUC was 0.7879 (*P*<0.0001, 95%CI: 0.6914-0.8844), the RON AUC was 0.8360 (*P*<0.0001, 95%CI: 0.7486-0.9234), the RIN AUC was 0.762 (*P*<0.0001, 95%CI: 0.6629-0.8610), the RIS AUC was 0.7821 (*P*<0.0001, 95%CI: 0.6853-0.8790), the ROS AUC was 0.6372 (*P*=0.0082, 95%CI: 0.5377-0.7367). RNFL-ST AUC

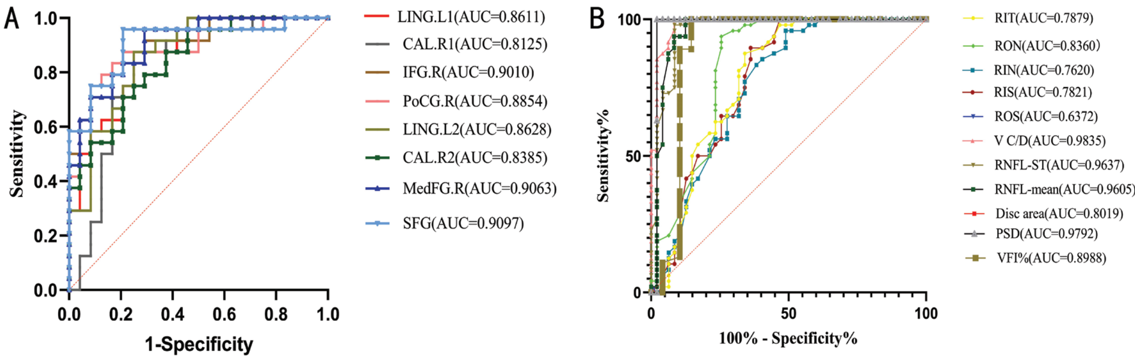

Figure 6 ROC curve analysis of ALFF changes in brain regions and clinical ophthalmic parameters ROC: Receiver operating characteristic; AUC: Area under the curve; ALFF: Amplitude of low-frequency fluctuations; LING.L1: Left lingual gyrus in slow-4 band; LING.L2: Left lingual gyrus in slow-5 band; CAL.R1: Right calcarine in slow-4 band; CAL.R2: Right calcarine in slow-5 band; IFG.R: Right inferior frontal gyrus; PoCG.R: Right postcentral gyrus; MedFG.R: Right medial frontal gyrus; SFG: Superior frontal gyrus; RIT: Inner temporal retina; RON: Outer nasal retina; RIN: Inner nasal retina; RIS: Inner superior retina; ROS: Outer superior retina; V C/D: Vertical cup-disc ratio; RNFL-ST: Retinal nerve fiber layer superior thickness; RNFL-mean: Mean retinal nerve fiber layer thickness; PSD: Pattern standard deviation; VFI: Visual field index.

was 0.9637 (P<0.0001, 95%CI: 0.9252-1.000), the RNFL-mean AUC was 0.9605 (P<0.0001, 95%CI:0.9153-1.000), the vertical C/D AUC was 0.9835 (P<0.0001, 95%CI: 0.9616-1.000), the disc area AUC was 0.8019 (P<0.0001, 95%CI: 0.7007-0.9031). PSD AUC was 0.9792 (P<0.0001, 95%CI: 0.9388-1.000), the VFI AUC was 0.8988 (P<0.0001, 95%CI: 0.8181-0.9794; Figure 6B). For the diagnosis of POAG, RNFL-ST, RNFL-Mean, PSD and vertical C/D performed the best, and ALFF showed better diagnostic performance than macular parameters.

DISCUSSION

Early-stage POAG is often missed because of the absence of obvious symptoms, and the lesion often progresses to the late stage by the time it is diagnosed. Current research and clinical practice are constantly attempting to identify more accurate and reliable diagnostic methods and standards to improve the rate and accuracy of the early diagnosis of POAG. To this end, we investigated the changes in frequency-dependent ALFF in POAG patients and HCs by rs-fMRI with the following objectives: 1) to explore the correlation between ALFF changes and ocular parameters in POAG patients and determine whether ALFF parameters can reflect the severity of POAG; 2) and to use fMRI imaging parameters of ALFF in different brain regions to diagnose POAG patients during follow-up.

Our study revealed that POAG patients exhibited abnormal spontaneous neural activity that can be detected in the early stages (Figure 2F), which is consistent with the findings of Wang *et al*[8] and Trivedi *et al*[25]. The abnormal changes in ALFF in mild POAG patients suggest that functional POAG changes may appear before organic changes, suggesting that ALFF analysis may be a method to detect early-stage POAG. Qing *et al*[26] suggested that attention should be shifted from alleviating POAG visual field defects to preventing further development of early or "normal" visual fields. The excellent retinal positioning ability of fMRI for the diagnosis of early POAG[27] makes it a suitable method for physiopathological studies of the visual pathway[28-29]. Although we found a corresponding trend in abnormal brain areas in worsening POAG patients, it was not statistically significant (Figure 2G).

In our study, ALFF alterations in POAG patients were mostly observed in the frontal lobe. According to the approach-withdrawal motivational/emotional model, left-sided frontal activity is assumed to be related to the approach system, which elicits positive emotion, approach-related motivation, and goal-directed behavior, whereas right-sided frontal activity is assumed to be associated with the withdrawal system, which elicits negative affect, withdrawal-related motivation and behavior[30]. On the basis of this model, greater right-sided frontal activity has been proposed as a risk factor for the development of affective disorders[31]. Wang *et al*[32] and Chen *et al*[33] reported functional impairments in the frontal cortex, and some regional functional changes were associated with altered ophthalmic clinical parameters. A decrease in frontal spontaneous neural activity may indicate dysfunction in visual stimulus processing, object recognition, and memory recall. Previous studies on ALFF revealed that patients with neovascular glaucoma had lower ALFF values in the left medial frontal gyrus (P<0.001) and higher ALFF values in the right superior and left middle frontal gyri than did HCs (P<0.001)[34]. However, Huang *et al*[35] reported that compared with HCs, primary angle-closure glaucoma patients had significantly lower ALFF values in the bilateral middle frontal gyrus and bilateral superior frontal gyrus, which may be related to differences in the pathogenesis of glaucoma. The ALFF value in the frontal lobe was also decreased in diabetic optic neuropathy patients, and some frontal lobe values were negatively correlated with anxiety scale and depression scale scores and ALFF values in the medial frontal gyrus[36]. Moreover, ALFF changes in this study occurred mostly in the right brain region, which may be related to the fact that the moderate to severe POAG patients included in this study had mostly left-eye involvement.

The visual cortical area is located in the upper and lower cortices of the occipital lobe, cuneus and lingual gyrus, and a reduction in spontaneous neural activity in these areas suggests damage to both the primary and higher visual cortex[37]. The LING.L is located at the interface of the occipital and temporal lobes, near the medial surface, and plays an important role in visual processing, especially in word recognition and reading, in addition to assisting memory and visual association[19]. In this study, the POAG ALFF values in this area were reduced, which suggests that POAG patients have potential impairments in visual processing and memory function. Compared with those in HCs, cerebral cortical changes in primary visual function in POAG patients were significantly associated with the degree of damage to the optic nerve and retina. Previous studies have also shown that in POAG patients, cerebral blood flow in the visual cortex, default mode network, and motor and sensory cortex decreases[32], and ALFF/fALFF values significantly decrease[37]. This study identified alterations in frontal and lingual regions, and we believe that these differences may reflect either different stages of disease progression or differences in research methods, such as frequency band selection and sample characteristics. In addition, morphology and volume changes and some brain changes are associated with the severity of POAG lesions[38]. Therefore, the use of fMRI to assess spontaneous neural activity in the visual cortex is a very promising method for objectively examining POAG.

In our study, in mild POAG patients and when we separately analyzed the correlation of ophthalmic parameters in the left eye with ALFF in abnormal brain regions and found an association of ALFF with MD values, this was not accidental in the neuroimaging studies of glaucoma. Kosior-Jarecka *et al*[39] reported that reduced lateral geniculate nucleus volume in open angle glaucoma patients was associated with RNFLT but not with MD or VFI%. However, when Minosse *et al*[40] used the functional connectivity disruption index as a biomarker of POAG disease severity, there were significant associations between all disruption indices and the VFI%, RNFLT, and macular ganglion cell layer. There are only a few studies on the correlation between POAG brain region changes and visual field defects; therefore, our study has significance. In this study, brain regions with differential ALFF values were significantly correlated with RNFLT, which also indicates that POAG brain region changes may be correlated with disease severity. ROC curve analysis revealed that the RNFL-ST, RNFL-mean, PSD and vertical C/D had the best diagnostic performance for POAG, whereas the MedFG.R, SFG, IFG.R, LING.L, CAL.R, the diagnostic performance was acceptable, and the diagnostic performance of the CAL.R is relatively poor, which may be because the CAL.R, which was related mostly to macular-related parameters, was correlated with PSD and VFI only in the early stage of POAG, and the diagnostic value of macular-related parameters was the worst according to the ROC curve analysis. However, previous studies have shown that changes in different brain regions in POAG are related to blood flow[32,41]. In our study, brain region changes in POAG patients were found to be associated with the degree of ILM-RPET injury. This may be because POAG is associated with a reduced blood supply, but the order of the two occurrences remains controversial.

Tonagel *et al*[42] reported specific changes in the loss of cpRNFL thickness between POAG, optic nerve sheath meningioma and sphenoid wing meningioma patients. They suggested that head MRI should be considered in patients with significantly reduced RNFLT in the temporal region to exclude optic nerve compression. In this study, we performed detailed partitioning of the ILM-RPET and correlated it with abnormal POAG brain regions. We found that changes in POAG brain regions were associated with ILM-RPET injury. Although it is impossible to conduct a characteristic analysis of the macular area of POAG to further explore the mechanism of POAG-related cerebral hemodynamic disorders due to our small sample size, this is the first study in which this ILM-RPET partition method has been applied to study ALFF changes on fMRI in POAG patients. Therefore, we believe that a correlation study of cpRNFL and ILM-RPET zoning in POAG patients may yield surprising findings.

There are several limitations to our study. First, this study has a small sample size, which may limit the general applicability of the ROC curve results, which need to be validated in independent cohorts, and the effects of individual variability and sex on the study results cannot be excluded. Second, emotion, levels of cognition, anxiety and depression all influence the MRI findings of POAG patients, but the patients recruited in this study did not undergo psychological tests. Third, this study failed to find a correlation between POAG eyes and changes in brain regions, but this may be related to the complex interaction mechanism in the left/right hemispheres. In future studies, the sample size will be expanded to include monocular POAG patients to obtain more accurate results. Finally, age is an important factor affecting changes in brain regions. In future studies, POAG brain region changes in different age groups could be studied to avoid the influence of age on the results.

In conclusion, current neuroimaging studies have shown that POAG may be a widespread neurodegenerative disease. Although it is still difficult to determine whether the spontaneous abnormal brain activity observed in POAG patients is the cause of the disease or results from the disease, functional neuroimaging using ALFF may have practical clinical significance for detecting early POAG lesions and disease progression.

ACKNOWLEDGEMENTS

Foundation: Supported by National Natural Science Foundation of China (No.82260203).

Conflicts of Interest: Huang Y, None; **Luo HD,** None; **Shu YQ,** None; **Ouyang F,** None; **Song YN,** None; **Wang YY,** None; **Yu XQ,** None; **Xiong C,** None; **Yang L,** None; **Zhang X,** None.

REFERENCES

1 Alqawlaq S, Flanagan JG, Sivak JM. All roads lead to glaucoma: induced retinal injury cascades contribute to a common neurodegenerative outcome. *Exp Eye Res* 2019;183:88-97.

2 Geyer O, Levo Y. Glaucoma is an autoimmune disease. *Autoimmun Rev* 2020;19(6):102535.

3 Jiang S, Kametani M, Chen DF. Adaptive immunity: new aspects of pathogenesis underlying neurodegeneration in glaucoma and optic neuropathy. *Front Immunol* 2020;11:65.

4 Zukerman R, Harris A, Oddone F, *et al*. Glaucoma heritability: molecular mechanisms of disease. *Genes* 2021;12(8):1135.

5 Baudouin C, Kolko M, Melik-Parsadaniantz S, *et al*. Inflammation in glaucoma: from the back to the front of the eye, and beyond. *Prog Retin Eye Res* 2021;83:100916.

6 Artero-Castro A, Rodriguez-Jimenez FJ, Jendelova P, *et al*. Glaucoma as a neurodegenerative disease caused by intrinsic vulnerability factors. *Prog Neurobiol* 2020;193:101817.

7 Vernazza S, Oddone F, Tirendi S, *et al*. Risk factors for retinal ganglion cell distress in glaucoma and neuroprotective potential intervention. *Int J Mol Sci* 2021;22(15):7994.

8 Wang Q, Qu X, Chen W, *et al*. Altered coupling of cerebral blood flow and functional connectivity strength in visual and higher order cognitive cortices in primary open angle glaucoma. *J Cereb Blood Flow Metab* 2021;41(4):901-913.

9 Li T, Qu X, Chen W, *et al*. Altered information flow and microstructure abnormalities of visual cortex in normal-tension glaucoma: evidence from resting-state fMRI and DKI. *Brain Res* 2020;1741:146874.

10 Nucci C, Garaci F, Altobelli S, *et al*. Diffusional kurtosis imaging of white matter degeneration in glaucoma. *J Clin Med* 2020;9(10):3122.

11 Colbert MK, Ho LC, van der Merwe Y, *et al*. Diffusion tensor imaging of visual pathway abnormalities in five glaucoma animal models. *Invest Ophthalmol Vis Sci* 2021;62(10):21.

12 Chan K, Kasi A, Faiq M. *In vivo* imaging of structural, metabolic and functional brain changes in glaucoma. *Neural Regen Res* 2019;14(3):446.

13 Chai Z, Yang B, Qu X, *et al*. Alterations in surface-based amplitude of low-frequency fluctuations primary open-angle glaucoma link to neurotransmitter profiling and visual impairment severity. *Brain Imag Behav* 2025;19(1):159-174.

14 Wang Y, Shu Y, Cai G, *et al*. Altered static and dynamic functional network connectivity in primary angle-closure glaucoma patients. *Sci Rep* 2024;14:11682.

15 Li T, Wang Q, Yang B, *et al*. Glymphatic system impairment in normal tension glaucoma evaluated by diffusion tensor image analysis along the perivascular space. *Brain Res* 2025;1850:149450.

16 Sekimitsu S, Xiang D, Smith SL, *et al*. Deep ocular phenotyping across primary open-angle glaucoma genetic burden. *JAMA Ophthalmol* 2023;141(9):891-899.

17 Angmo D, Kapoor A, Warjri GB, *et al*. Comparative evaluation of OCT with OCTA changes at the optic disc and macula in glaucoma suspect and early glaucoma. *Indian J Ophthalmol* 2025;73(Suppl 2):S260-S266.

18 Tejavibulya L, Peterson H, Greene A, *et al*. Large-scale differences in functional organization of left- and right-handed individuals using whole-brain, data-driven analysis of connectivity. *NeuroImage* 2022;252:119040.

19 Li XT, Chen L, Wang XM, *et al*. Differences in cerebral spontaneous neural activity correlate with gene-specific transcriptional signatures in primary angle-closure glaucoma. *Neuroscience* 2025;565:399-419.

20 Rao A, Singh AK, Mukherjee S, *et al*. Comparing focal and global responses on multifocal electroretinogram with retinal nerve fibre layer thickness by spectral domain optical coherence tomography in glaucoma. *Br J Ophthalmol* 2015;99(4):500-507.

21 Sakaguchi K, Higashide T, Udagawa S, *et al*. Comparison of sectoral structure-function relationships in glaucoma: vessel density versus thickness in the peripapillary retinal nerve fiber layer. *Invest Ophthalmol Vis Sci* 2017;58(12):5251.

22 Lian Y, Lu W, Xu A, *et al*. The correlation between modifications to corneal topography and changes in retinal vascular density and retinal thickness in myopic children after undergoing orthokeratology. *Front Med* 2023;10:1166429.

23 Jiang F, Yu C, Zuo MJ, *et al*. Frequency-dependent neural activity in primary angle-closure glaucoma. *Neuropsychiatr Dis Treat* 2019;15:271-282.

24 Grassi L, Salazar Vega D, De Gainza A, *et al*. Phenotypic expressions of the optic disc in primary open-angle glaucoma. *Eye(Lond)* 2023;37(18):3839-3846.

25 Trivedi V, Bang JW, Parra C, *et al*. Widespread brain reorganization perturbs visuomotor coordination in early glaucoma. *Sci Rep* 2019;9:14168.

26 Qing G, Zhang S, Wang B, *et al*. Functional MRI signal changes in primary visual cortex corresponding to the central normal visual field of patients with primary open-angle glaucoma. *Invest Ophthalmol Vis Sci* 2010;51(9):4627.

27 Sun Y, Huang W, Li F, *et al*. Subcortical visual pathway may be a new way for early diagnosis of glaucoma. *Med Hypotheses* 2019;123:47-49.

28 Heitmann C, Zhan M, Linke M, *et al*. Early visual experience refines the retinotopic organization within and across visual cortical regions. *Curr Biol* 2023;33(22):4950-4959.e4.

29 Ribeiro FL, York A, Zavitz E, *et al*. Variability of visual field maps in human early extrastriate cortex challenges the canonical model of organization of V2 and V3. *eLife* 2023;12:e86439.

30 Zhang J, Zamoscik VE, Kirsch P, *et al*. No evidence from a negative mood induction fMRI task for frontal functional asymmetry as a suitable neurofeedback target. *Sci Rep* 2023;13:17557.

31 van der Vinne N, Vollebregt MA, van Putten MJAM, *et al*. Frontal alpha asymmetry as a diagnostic marker in depression: fact or fiction? A meta-analysis. *Neuroimage Clin* 2017;16:79-87.

32 Wang Q, Qu X, Wang H, *et al*. Arterial spin labeling reveals disordered cerebral perfusion and cerebral blood flow-based functional connectivity in primary open-angle glaucoma. *Brain Imag Behav* 2024;18(1):231-242.

33 Chen L, Li S, Cai F, *et al*. Altered functional connectivity density in primary angle-closure glaucoma patients at resting-state. *Quant Imaging Med Surg* 2019;9(4):603-614.

34 Peng ZY, Liu YX, Li B, *et al*. Altered spontaneous brain activity patterns in patients with neovascular glaucoma using amplitude of low-frequency fluctuations: a functional magnetic resonance imaging study. *Brain Behav* 2021;11(3):e02018.

35 Huang X, Zhong YL, Zeng XJ, *et al*. Disturbed spontaneous brain activity pattern in patients with primary angle-closure glaucoma using amplitude of low-frequency fluctuation: a fMRI study. *Neuropsychiatr Dis Treat* 2015;11:1877-1883.

36 Wang XY, Xu SH, Wei H, *et al*. Amplitude of low-frequency fluctuation to determine disturbed spontaneous brain-activity pattern in patients with diabetic optic neuropathy. *Diabetes Metab Syndr Obes* 2023;16:2899-2909.

37 Li T, Liu Z, Li J, *et al*. Altered amplitude of low-frequency fluctuation in primary open-angle glaucoma: a resting-state FMRI study. *Invest Ophthalmol Vis Sci* 2014;56(1):322-329.

38 Fukuda M, Omodaka K, Tatewaki Y, *et al*. Quantitative MRI evaluation of glaucomatous changes in the visual pathway. *PLoS One* 2018;13(7):e0197027.

39 Kosior-Jarecka E, Pankowska A, Polit P, *et al*. Volume of lateral geniculate nucleus in patients with glaucoma in 7Tesla MRI. *J Clin Med* 2020;9(8):2382.

40 Minosse S, Garaci F, Martucci A, *et al*. Primary open angle glaucoma is associated with functional brain network reorganization. *Front Neurol* 2019;10:1134.

41 Promelle V, Bouzerar R, Daouk J, *et al*. Ophthalmic artery and superior ophthalmic vein blood flow dynamics in glaucoma investigated by phase contrast magnetic resonance imaging. *J Glaucoma* 2021;30(1):65-70.

42 Tonagel F, Wilhelm H, Kelbsch C, *et al*. Characteristics of peripapillary retinal nerve fiber layer atrophy in glaucoma, optic nerve sheath meningioma, and sphenoid wing meningioma. *Graefes Arch Clin Exp Ophthalmol* 2022;260(2):577-581.